Laser step-heating $^{40}Ar/^{39}Ar$ analyses of biotites from meta-granites in the UHP Brossasco-Isasca Unit of Dora-Maira Massif, Italy

Tetsumaru ITAYA[*,**], Hironobu HYODO[***], Takeshi IMAYAMA[***] and Chiara GROPPO[†,‡]

[*]*Institute of Geohistory, Japan Geochronology Network, Akaiwa 701-2503, Japan*
[**]*Hiruzen Institute for Geology and Chronology, Co., Ltd., Okayama 703-8252, Japan*
[***]*Research Institute of Natural Sciences, Okayama University of Science, Okayama 700-0005, Japan*
[†]*Department of Earth Sciences, University of Torino, 10125 Torino, Italy*
[‡]*IGG-CNR, Via Valperga Caluso 35, I-10125 Torino, Italy*

Two undeformed metagranite samples were collected from the UHP Brossasco-Isasca Unit (BIU) of Dora-Maira Massif, Italy to carry out the laser step-heating $^{40}Ar/^{39}Ar$ analyses of individual biotite crystals. The metagranites occur as undeformed domains (m- to ten of meters in size) within strongly deformed augen-gneiss. They still preserve their medium- to coarse- grained igneous texture and are composed mainly of K-feldspar, plagioclase pseudomorph, quartz, and biotite that preserve their original igneous shape but are either re-equilibrated or replaced by new phases.

Three biotite crystals from the first sample have similar age spectra showing 400 to 300 Ma, except for the first fraction (500-1500 Ma). On the contrary, the age spectra of five biotite crystals from the second sample are significantly different; these biotites show saddle shape $^{40}Ar/^{39}Ar$ age spectra, except for one crystal. The oldest fractions have ages (800 to 1300 Ma) three to four times older than that of the granite protolith (which is late Permian). This extremely high intensity of excess argon could be due to an 'Excess-Argon Wave' (EAW) phenomenon, occurred during the quick exhumation of the BIU, combined with the extremely short ductile deformation history. The observed variation of the biotite age spectra may reflect the different trapping processes of EAW and/or localized source of EAW.

Keywords: Western Alps, Dora-Maira Massif, Brossasco-Isasca UHP unit, Permian metagranite, Biotite $^{40}Ar/^{39}Ar$ age, Excess-Argon Wave

INTRODUCTION

K-Ar ($^{40}Ar/^{39}Ar$) analyses of phengitic micas from HP-UHP metamorphic rocks from the Dora-Maira Massif (Italian western Alps) yield a wide variation of K-Ar ($^{40}Ar/^{39}Ar$) ages ranging from 25 to 320 Ma (cf. Scaillet et al., 1990; Monié and Chopin, 1991; Scaillet et al., 1992; Arnaud and Kelley, 1995; Hammerschmidt et al., 1995; Scaillet, 1996; Di Vincenzo et al., 2006; Schertl and Hammerschmidt, 2016). Similar discordant and geologically meaningless ages have been also reported from poly-metamorphic rocks from many collisional settings (Chopin and Maluski 1980; Tonarini et al. 1993; Li et al. 1994; Sherlock and Arnaud 1999; Giorgis et al. 2000; De Jong et al. 2001; Jahn et al. 2001; Gouzu et al., 2006; Itaya et al. 2009; Beltrando et al. 2013; Halama et al. 2014). This type of excess argon is due to the fact that white micas in continental lithologies consisting of precursor older rocks, have not been reset completely during the MP-HP-UHP metamorphism, because the closure temperature of white mica is much higher than that currently generally accepted, being ~ 600 °C (cf. Itaya et al., 2009; Gouzu et al., 2016).

Biotite also has complicated excess argon behavior in thermally overprinted rocks near tectonic contacts (Wanless et al., 1970) and/or in contact aureoles (Hyodo and York, 1993). For example, Hyodo and York (1993) found significantly old 'discordant' biotite $^{40}Ar/^{39}Ar$ ages, older than the age of the hosting lithology, in a narrow

doi:10.2465/jmps.171201
T. Itaya, tetsumaru.itaya@gmail.com Corresponding author

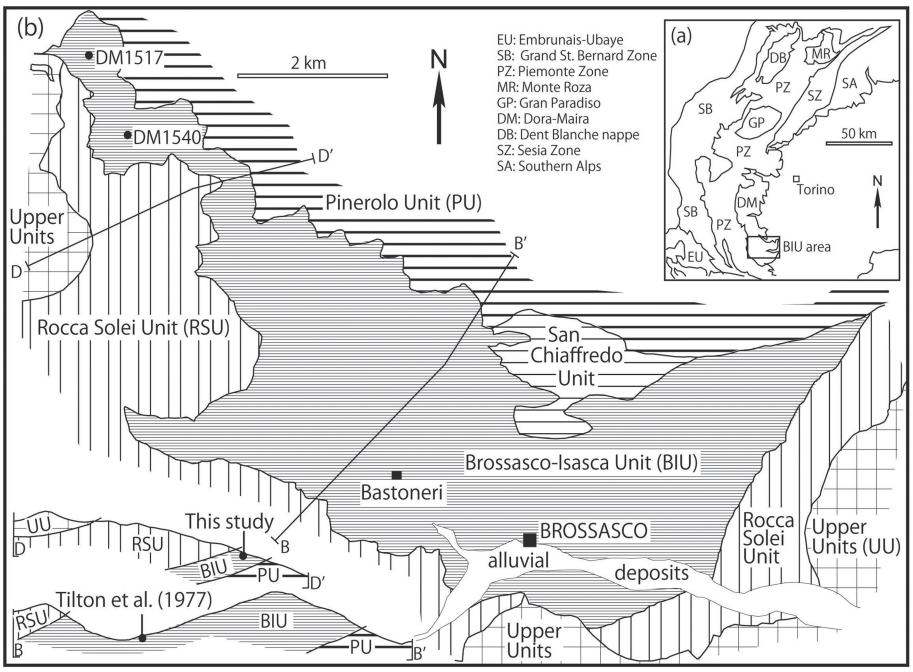

Figure 1. Geological sketch map of the UHP Brossasco-Isasca Unit (southern Dora-Maira Massif, Italy), modified from Compagnoni et al. (2012). Solid circles show the location of the analyzed samples (DM1517 and DM1540), that are undeformed metagranites preserved within strongly deformed augen gneiss. The circles in the cross sections show the location of samples studied in this paper and of those studied by Tilton et al. (1997).

zone of a contact aureole and called this phenomenon 'argon wave (Argonami)'. This type of excess ^{40}Ar was incorporated into biotite by diffusion. Itaya et al. (2009) and Itaya and Tsujimori (2015) later named the same phenomenon as 'Excess-Argon Wave'. Since then, the phenomenon of the trapping of 'Excess-Argon Wave' by minerals has been increasingly observed in biotite, kyanite, white mica, and K-feldspar from many types of lithologies (Itaya et al., 2005, 2009; Itaya and Tsujimori, 2015; Itaya et al., 2017).

During the laser step-heating $^{40}Ar/^{39}Ar$ analyses of individual biotite crystals from metagranite in the UHP Brossasco-Isasca Unit of Dora-Maira Massif, Italy, we obtained ages three to four orders of magnitude older than that of the granite protolith (which is late Permian: e.g., Gebauer et al., 1997). In this study, we describe laser step heating $^{40}Ar/^{39}Ar$ analyses of biotite crystals from two metagranite samples with the aim of revealing how the biotite acquired the extremely large amount of excess argon. Based on the literature, we discuss in detail the 'Excess-Argon Wave' hypothesis as well as the source and the trapping processes of the 'Excess-Argon Wave' in the UHP Brossasco-Isasca Unit of Dora-Maira Massif, Italy.

SAMPLE DESCRIPTION

The Dora-Maira Massif (DMM) is one of the Internal Crystalline Massifs of the Penninic Domain of the western Alps, together with the Monte Rosa and the Gran Paradiso massifs. The southern part of DMM is composed of the following four main tectonometamorphic units, from the lower to the upper structural levels: the Pinerolo, San Chiaffredo, Brossasco-Isasca and Rocca Solei units (Fig. 1). The UHP Brossasco-Isasca Unit (BIU) consists of a Variscan amphibolite-facies metamorphic basement (now garnet-kyanite phengitic micaschist, with minor intercalations of impure marble and eclogite) intruded by Permian granitoids (now mainly augen-gneiss, minor metagranite, and pyrope-bearing whiteschist) which produced a locally preserved contact metamorphic aureole (Compagnoni et al., 2012). The UHP stage in the BIU was described by Gebauer et al. (1997) and Duchêne et al. (1997). Gebauer et al. (1997) gave U-Pb SHRIMP zircon average age of 35.4 ± 1.0 Ma, obtained from different rock types and Duchêne et al. (1997) reported Lu-Hf age of 32.8 ± 1.2 Ma, which was obtained on a garnet-whole rock pair from a pyrope-bearing whiteschist. Rubatto and Hermann (2001) carried out SHRIMP U-Pb analyses of single growth zones of titanite grains from two calc-silicate nodules in marbles, providing a mean age of 35.1 ± 0.9 Ma. Di Vincenzo et al. (2006) provided a Rb-Sr internal isochron age of 36.28 ± 0.33 Ma using omphacite, phengites, and whole rock from an eclogite.

The undeformed metagranite samples (DM1517 and DM1540), collected from the northwestern part of BIU (Fig. 1), still preserve the original medium- to coarse-grained igneous texture: they are composed mainly of K-feldspar, plagioclase pseudomorph, quartz, biotite (Fig. 2A), and accessory ilmenite. Quartz, plagioclase pseudomorph, K-feldspar, and biotite preserve their original

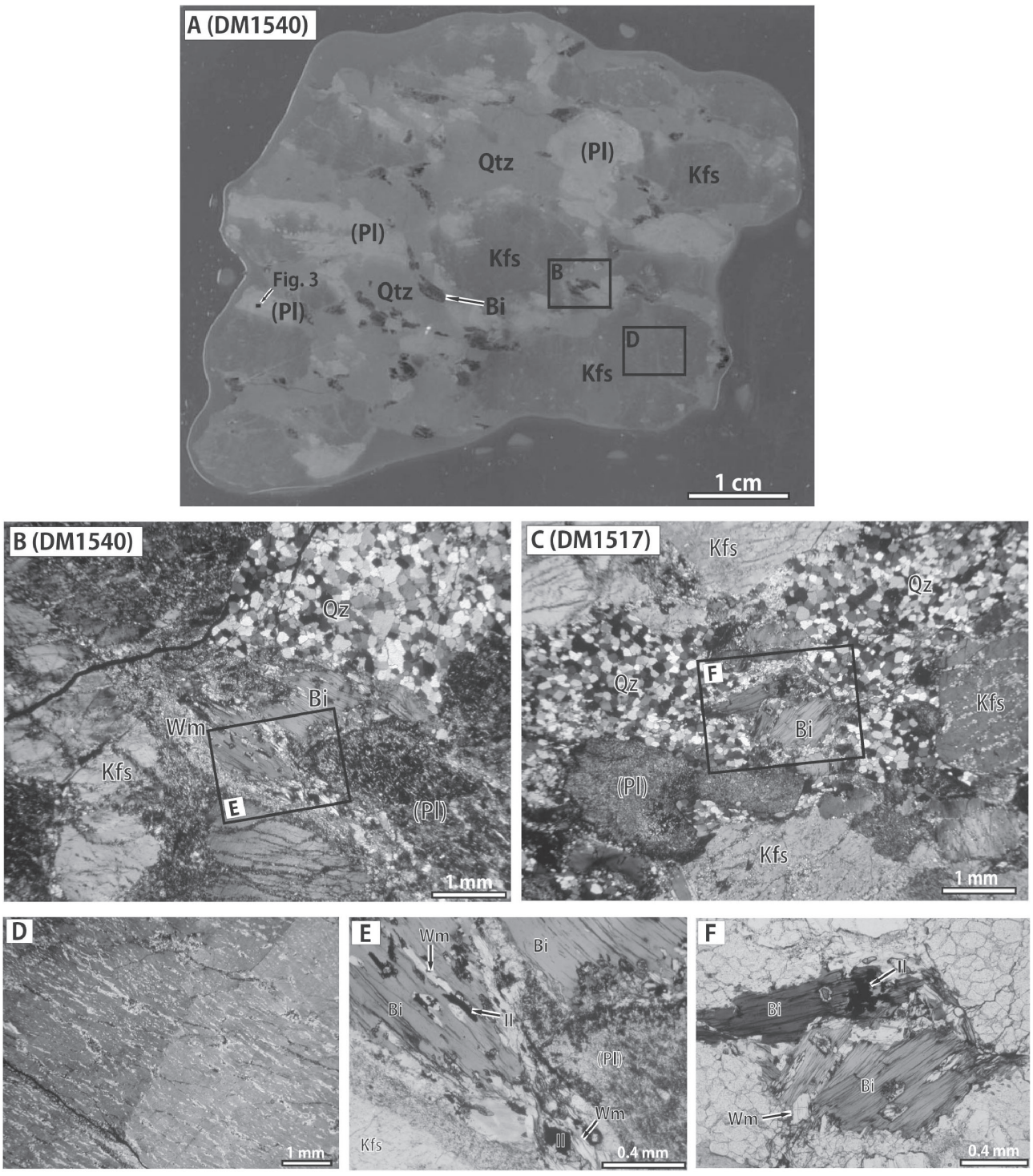

Figure 2. Showing a scanned image and photomicrographs of the metagranite samples (DM1517 and DM1540). (A) is a scanned image of a thin section of DM1540, showing the still preserved undeformed igneous texture. The insets show the areas of photomicrograph in (B) and (D), and of BSE image by EMP (Fig. 3). (B) and (C) are the photomicrographs of DM1540 and DM1517, respectively. Quartz occurs as fine-grained granoblastic aggregate, statically derived from inversion of coesite. Plagioclase pseudomorph (Pl) with igneous crystal shape is composed of a fine-grained aggregate including albite and zoisite (or epidote), and minor titanite, phengite, and apatite. Biotite is surrounded and partly replaced by fine-grained white mica. The insets show the areas of photomicrograph of (E) and (F). (D) is the photomicrograph of the inset shown in (A), showing the perthitic nature of K-feldspar. Light and dark portions are albite and orthoclase, respectively. (E) and (F) are the photomicrographs of the insets shown in (B) and (C), respectively, showing ilmenite closely associated with biotite. Kfs, K-feldspar; (Pl), plagioclase pseudomorph; Qtz, quartz; Bt, biotite; Wm, white mica; Il, ilmenite. Color version is available online from https://doi.org/10.2465/jmps.171201.

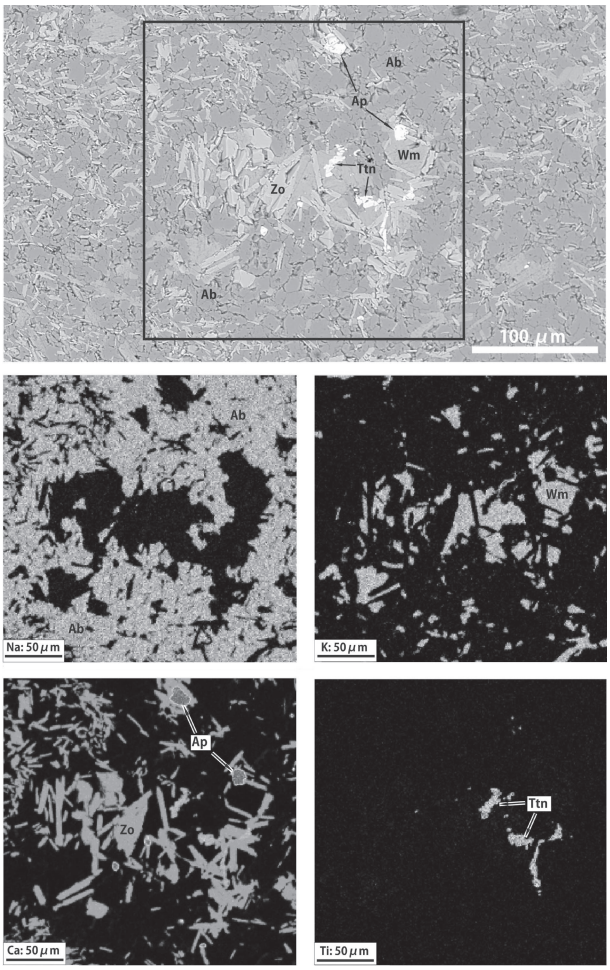

Figure 3. BSE image and elemental maps of the very small area indicated by a point in Figure 2A. Ab, albite; Zo, zoisite; Wm, white mica; Ttn, titanite; Ap, apatite. Color version is available online from https://doi.org/10.2465/jmps.171201.

igneous shape but are either re-equilibrated or replaced by new phases. Quartz occurs as a fine-grained granoblastic aggregate, statically derived from inversion of coesite (Compagnoni et al., 2012; Itaya et al., 2017; Figs. 2B and 2C). Plagioclase is now replaced by a fine-grained (tens of microns) aggregate (Figs. 2B and 2C), mainly consisting of albite and zoisite (or epidote), and minor titanite, phengite, and apatite, which have been identified by electron microprobe analyses (Fig. 3). K-feldspar occurs often as a perthite, especially in DM1540 (Fig. 2D). The perthitic exsolutions were likely formed during cooling of the Permian granite, while it intruded into the Variscan metamorphic basement. Biotite is surrounded and partly replaced by fine-grained white mica (Compagnoni et al., 2012; Itaya et al., 2017; Figs. 2B, 2C, 2E, and 2F). Ilmenite is closely associated with biotite (Figs. 2E and 2F).

Chemical compositions of constituent minerals were determined using a JXA-8230 electron microprobe (EMP) at Okayama University of Science. The operating conditions were 15 kV accelerating voltage, a 12 nA beam current, and 3 μm beam spot size. Natural and synthetic silicates and oxides were used as standard for calibration. Matrix corrections were performed using the ZAF quantitative correction calculation for oxides. Representative analyses of constituent minerals are shown in Table 1. EMP analyses revealed that K-feldspar has 94-97 mol% of orthoclase component. Biotite has Fe/(Fe + Mg) of 0.65-0.73, Al = 2.8-3.0 and Ti = 0.15-0.25 (a.p.f.u. on the basis of 11 oxygens). The fine-grained phengitic white mica replacing biotite is phengite with Si = 3.2-3.4 (a.p.f.u. on the basis of 11 oxygens) and are therefore likely related to the Alpine HP-UHP metamorphism. Albite in the perthite and in the plagioclase pseudomorph has a nearly pure composition (Table 1). Samples DM1517 and DM1540 have similar mineral chemistries for K-feldspar, albite, white mica, and biotite.

LASER STEP-HEATING $^{40}Ar/^{39}Ar$ ANALYSES

$^{40}Ar/^{39}Ar$ analyses of individual biotite crystals were carried out with the step-heating method in which the temperature ranges are from ~ 500 to ~ 1300 °C. Each grain (~ 0.5 mm in size) was placed in a 2 mm drill hole on an aluminum tray together with an age standard grain (3gr hornblende; Roddick, 1983), and calcium ($CaSi_2$) and potassium (synthetic $KAlSi_3O_8$ glass) compounds for Ca and K corrections. Subsequently the trays were vacuum-sealed in a quartz tube. Neutron irradiation of the sample was carried out in the core of 5 MW Research Reactor at Kyoto University (KUR) for 24 hours. The fast neutron flux density is 3.9×10^{13} n/cm^2/s and is confirmed to be uniform in the dimension of the sample holder ($\phi 16 \times 15$ mm), as little variation in J-values of the evenly spaced age standards was observed (Hyodo et al., 1999). Averaged J-values, potassium, and calcium correction factors are shown in Supplementary Table (available online from https://doi.org/10.2465/jmps.171201). Each biotite crystal was analyzed by the step-heating technique using a 5 W continuous argon ion laser. Temperatures of the samples were monitored by an infrared thermometer with a precision of 3 °C within an area of 0.3 mm diameter (Hyodo et al., 1995). Heating time at a laser power was set at 30 s. The extracted gas was purified with a SAES Zr-Al getter (St 101) and kept at 400 °C for 5 min. Argon isotopes were measured using the custom-made mass spectrometer with a high resolution ([M/ΔM] larger than 400), which allows separating hydrocarbon peaks except for mass 36 (Hyodo et al., 1994). Typical blanks of extraction lines are shown in Supplementary Table.

Table 1. Representative chemical compositions of constituent minerals obtained by EMP

Sample	DM1540								
Mineral	Kfs	Kfs	Ab	Ab	Wm	Wm	Bt	Bt	Zo
SiO_2	65.03	64.92	69.28	70.06	50.69	49.36	36.48	37.60	40.97
TiO_2	0.05	0.00	0.00	0.05	0.28	0.16	4.17	2.84	0.03
Al_2O_3	17.33	17.36	18.50	18.79	30.13	32.55	14.13	15.02	30.50
FeO	0.00	0.00	0.00	0.02	3.02	2.64	22.77	21.36	0.43
MnO	0.01	0.00	0.00	0.00	0.01	0.00	0.12	0.11	0.00
MgO	0.00	0.00	0.01	0.00	1.45	1.21	6.18	6.42	0.01
CaO	0.03	0.07	0.30	0.45	0.02	0.01	0.01	0.01	24.06
Na_2O	0.40	0.69	11.46	11.15	0.11	0.15	0.03	0.02	0.01
K_2O	17.33	17.00	0.17	0.17	10.66	10.78	10.01	9.76	0.04
Total	100.19	100.03	99.71	100.68	96.37	96.87	93.91	93.13	96.06
	O=8	O=8	O=8	O=8	O=11	O=11	O=11	O=11	O=12.5
Si	3.02	3.02	3.03	3.03	3.35	3.24	2.89	2.96	3.16
Al	0.95	0.95	0.95	0.96	2.34	2.52	1.32	1.39	2.77
Ti	0.00	0.00	0.00	0.00	0.01	0.01	0.25	0.17	0.00
Fe^{3+}	-	-	-	-	-	-	-	-	0.03
Fe^{2+}	0.00	0.00	0.00	0.00	0.17	0.15	1.51	1.41	-
Mn	0.00	0.00	0.00	0.00	0.00	0.00	0.01	0.01	0.00
Mg	0.00	0.00	0.00	0.00	0.14	0.12	0.73	0.75	0.00
Ca	0.00	0.00	0.01	0.02	0.00	0.00	0.00	0.00	1.99
Na	0.04	0.06	0.97	0.94	0.01	0.02	0.01	0.00	0.00
K	1.03	1.01	0.01	0.01	0.90	0.90	1.01	0.98	0.00
Total	5.04	5.04	4.98	4.96	6.92	6.96	7.73	7.67	7.95
X_{Ab}	0.03	0.06	0.98	0.97					
X_{An}	0.00	0.00	0.01	0.02					
X_{Or}	0.97	0.94	0.01	0.01					
X_{Fe}							0.67	0.65	

X_{Ab} = Na/(Ca + Na + K). X_{An} = Ca/(Ca + Na + K). X_{or} = K/(Ca + Na + K). X_{Fe} = Fe/(Fe + Mg).
Kfs, K-feldspar; Ab, albite; Bt, biotite; Wm, white mica; Zo, zoisite; Ep, epidote.

Results of step-heating analyses are shown in Supplementary Table. Age spectra and $^{37}Ar_{Ca}/^{39}Ar_K$ ratios of each crystal are displayed in Figure 4. The three biotite crystals from DM1517 have similar age spectra showing 400 to 300 Ma except for the first fraction (500-1500 Ma). The age spectra of five biotite crystals from DM1540 are significantly different from those of DM1517 because the crystals Bt1, Bt2, Bt4, and Bt5 show saddle-type spectra. The oldest fraction reaches 1200-1300 Ma (crystals Bt2, Bt3, and Bt5), being four times older than the metagranite protolith (late Permian). The oldest fraction of ages for the crystal Bt1 and Bt4 are three times older than the metagranite protolith.

DISCUSSION

Excess-Argon Wave hypothesis

The phenomenon of the trapping of the excess-argon by minerals through argon diffusion was proposed first by Hyodo and York (1993). They found significantly old 'discordant' biotite $^{40}Ar/^{39}Ar$ ages, older than the age of host lithology, in a narrow zone of a contact aureole and called this phenomenon 'argon wave (Argonami)' that was renamed 'Excess-Argon Wave' (EAW) by Itaya et al. (2009). The phenomenon of the trapping of EAW by minerals has been increasingly observed, also in regional metamorphic sequences. In the Barrovian-type metamorphic complex of the Longmenshan orogen (eastern Tibet), for example, some kyanite-grade metapelites yielded biotite $^{40}Ar/^{39}Ar$ ages 4 to 5 times older than those in the associated sillimanite-grade metapelites (Itaya et al., 2009); the excess ^{40}Ar was incorporated in biotite by diffusion through the breakdown reaction of muscovite with a significant amount of radiogenic argon. Another example is represented by some kyanite grains from the river sand in NE Japan, which gave extremely old Ar-Ar ages (8-6 Ga: Itaya et al., 2005). These very old ages have been interpreted as due to the fact that kyanite recrystallized in the host rocks under ultra-high argon pressure derived from

Table 1. (Continued)

Sample	D1517							
Mineral	Kfs	Ab	Ab	Wm	Wm	Bt	Bt	Ep
SiO_2	63.82	67.66	65.73	49.09	48.04	35.20	34.59	37.93
TiO_2	0.01	0.00	0.00	0.41	0.85	2.49	3.56	0.00
Al_2O_3	18.85	20.92	21.53	30.99	31.18	15.94	15.88	28.43
FeO	0.02	0.02	0.00	3.53	3.93	25.84	25.93	6.29
MnO	0.00	0.00	0.00	0.00	0.00	0.19	0.18	0.00
MgO	0.00	0.02	0.02	1.73	1.46	5.65	5.36	0.02
CaO	0.05	0.96	1.82	0.01	0.02	0.00	0.00	22.74
Na_2O	0.67	11.04	10.87	0.19	0.17	0.10	0.08	0.00
K_2O	15.79	0.08	0.09	10.31	10.51	8.94	9.13	0.00
Total	99.21	100.69	100.05	96.25	96.17	94.36	94.72	95.40
	O=8	O=8	O=8	O=11	O=11	O=11	O=11	O=12.5
Si	2.97	2.94	2.89	3.26	3.21	2.80	2.75	2.99
Al	1.03	1.07	1.11	2.42	2.45	1.49	1.49	2.64
Ti	0.00	0.00	0.00	0.02	0.04	0.15	0.21	0.00
Fe^{3+}	-	-	-	-	-	-	-	0.41
Fe^{2+}	0.00	0.00	0.00	0.20	0.22	1.72	1.72	-
Mn	0.00	0.00	0.00	0.00	0.00	0.01	0.01	0.00
Mg	0.00	0.00	0.00	0.17	0.15	0.67	0.64	0.00
Ca	0.00	0.05	0.09	0.00	0.00	0.00	0.00	1.92
Na	0.06	0.93	0.93	0.02	0.02	0.02	0.01	0.00
K	0.94	0.01	0.01	0.87	0.90	0.91	0.93	0.00
Total	5.01	4.99	5.02	6.96	6.98	7.76	7.76	7.97
X_{Ab}	0.06	0.95	0.91					
X_{An}	0.00	0.05	0.08					
X_{Or}	0.94	0.00	0.00					
X_{Fe}						0.72	0.73	

X_{Ab} = Na/(Ca + Na + K). X_{An} = Ca/(Ca + Na + K). X_{or} = K/(Ca + Na + K). X_{Fe} = Fe/(Fe + Mg).
Kfs, K-feldspar; Ab, albite; Bt, biotite; Wm, white mica; Zo, zoisite; Ep, epidote.

radiogenic argon in potassium-rich phases such as phengites during the Barrovian type retrogression of UHP rocks. Similarly, the excess ^{40}Ar bearing phengite ages obtained for the Gongen eclogite in the Sanbagawa belt, SW Japan, might suggest a phenomenon similar to an EAW (Itaya and Tsujimori, 2015), because the excess ^{40}Ar was not inherited from precursor older rocks. In this case, it has been demonstrated that the excess ^{40}Ar preserved in the Gongen eclogite formed by the interaction between metagreywacke and metaperidotite with mantle-derived noble gas (very-high $^{40}Ar/^{36}Ar$ ratio of 3500-8000; cf. Kaneoka and Takaoka, 1980) at eclogite-facies depth. Fluid exchange between deep-subducted sediments and mantle material might have enhanced the gain of mantle-derived extreme ^{40}Ar in the metasediments. The high argon pressure environment created by the interaction between metasediments, peridotite and fluids would have allowed the trapping of a large amount of excess argon within phengitic micas. Recently, Itaya et al. (2017) reported excess argon bearing K-feldspar from metagranite in the UHP Brossasco-Isasca Unit of Dora-Maira Massif, Italy, and pointed out the possibility that the K-feldspar has trapped EAW generated by the argon release from micas during exhumation and cooling of the host lithologies. Thus, instead of total or partial resetting of the original age, the phenomenon of the trapping of the excess-argon by minerals through argon diffusion may be quite common in polymetamorphic MP-HP-UHP metamorphic rocks, depending on the closure temperature of minerals and on the presence of transient argon pressure. In particular, biotites older than the hosting rocks must be related to EAW generated by the argon release from micas during exhumation and cooling of the hosting lithologies and/or by heating of the country rocks induced by intrusive rocks.

Possible source of EAW in the Dora-Maira Massif

The EAW observed in the studied biotite crystals could have been generated during exhumation and cooling of

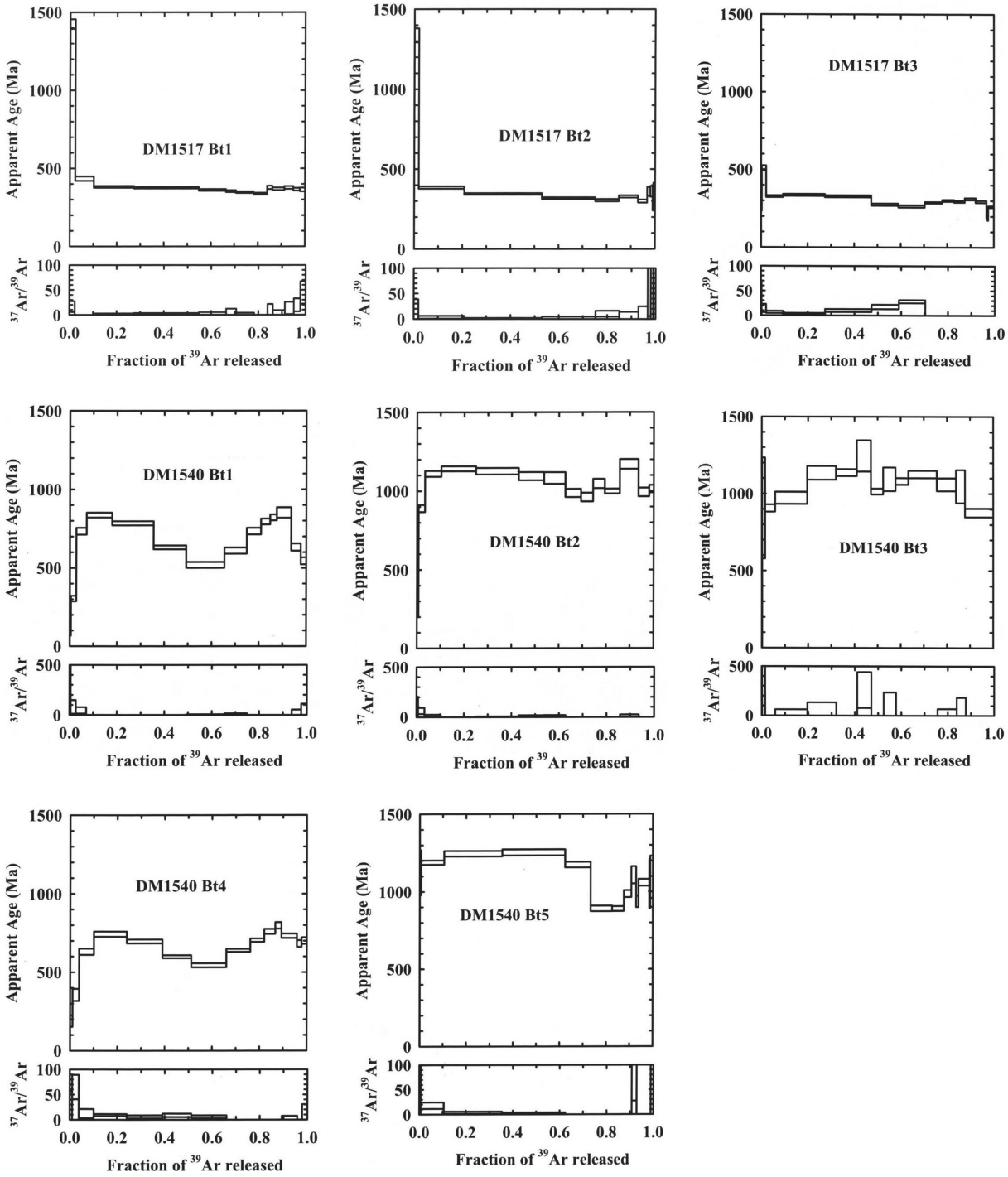

Figure 4. Age spectra and $^{37}Ar_{Ca}/^{39}Ar_K$ ratios of biotite crystals from DM1517 and DM1540 by the laser step-heating analyses.

the lithologies surrounding the metagranite as described below. The metagranite investigated in this study occurs as undeformed domains (m- to ten of meters in size) within strongly deformed augen-gneiss (Compagnoni et al., 2012), thus suggesting that it escaped the pervasive deformation associated to the exhumation of the BIU. In contrast, the white micas of both the augen-gneiss and the pyrope-bearing whiteschist hosting the metagranite experienced ductile deformation during exhumation. This ductile deformation could have enhanced argon release from white micas with radiogenic argon, as already documented in previous phengite K-Ar (Ar-Ar) geochronological studies of HP-UHP metamorphic rocks (cf. Itaya et al., 2011; Gouzu et al., 2016). The studied biotite crys-

tals from the metagranite could have trapped the EAW generated by the argon release from the white micas of the hosting lithologies, deformed during exhumation of the BIU.

Tilton et al. (1997) carried out the $^{40}Ar/^{39}Ar$ analyses of the biotite separates from similar undeformed metagranites collected near Bastoneri, 7–9 km SE of the sites of the samples DM1540 and DM1517. Their age spectra are complicated, having the troughs between 900–971 °C and the age variation from 70 to 215 Ma, younger than the granite protolith (late Permian). The BIU has experienced the HP–UHP Alpine evolution (peak *P*–*T* conditions at 4.2 GPa, 730 °C, e.g., Ferrando et al., 2009 and references therein). This suggests that the biotites in the metagranites should have been reset, as concerning the K–Ar system, during the Alpine evolution and could trap the EAW generated during exhumation of the BIU, arising the problem of explaining why the biotites from the metagranites analysed by Tilton et al. (1997) are much younger than those from the metagranites (DM 1517 and DM 1540) in the northwestern part of the BIU. This difference may be due to the fact that the metagranites analysed by Tilton et al. (1997) were far from the source of EAW in comparison with the studied metagranites (DM 1517 and DM 1540).

Three possible sources of EAW can be envisaged:

(1) The first possible source of EAW could be the garnet + kyanite–bearing phengitic micaschists of the Variscan basement in which the metagranite was intruded (i.e., Polymetamorphic Complex: Compagnoni et al., 2012). It has been demonstrated that kyanite can retain extreme amounts of excess argon (Itaya et al., 2005), therefore EAW could derive from the breakdown of kyanite during exhumation.

(2) A second possible source of EAW would be the underlying Pinerolo Unit (epidote–blueschist metamorphic overprint), which experienced peak temperature much lower (*T*; ~ 400 °C, *P*; ~ 0.8 GPa) (Chopin et al., 1991; Avigad et al., 2003) than that of the BIU. Having experienced peak metamorphism under epidote–blueschist facies conditions, the Pinerolo Unit could have not been reset for its white mica K–Ar system during the Alpine metamorphism and could have preserved large amounts of radiogenic ^{40}Ar formed by the ^{40}K decay in micas.

(3) Another possible source may be the overlying Rocca Solei Unit (quartz–eclogite metamorphic overprint), which also experienced lower peak–*T* conditions than those experienced by the BIU (*T*; ~ 550 °C, *P*; ~ 1.5 GPa: Chopin et al., 1991; Matsumoto and Hirajima, 2000). In either case, the argon release could have been enhanced by the pervasive deformation occurred during exhumation. The two metagranite samples of this study (DM 1517 and DM 1540) have been collected from the narrow NW termination of the BIU, significantly closer to both the Pinerolo and the Rocca Solei Units in comparison with the metagranites studied by Tilton et al. (1997) (see the cross sections of Fig. 1). Further studies are required in order to understand which was the major source of EAW (i.e., BIU Polymetamorphic Complex versus Pinerolo Unit versus Rocca Solei Unit); this would require biotite Ar–Ar analyses from metagranites collected systematically from the whole BIU.

The studied metagranites (DM1517 and DM1540) have significantly different age spectra. The similar age spectra observed for the three biotite crystals from sample DM1517 suggest a homogeneous EAW trapping process for this sample. However, four of the five biotite crystals (crystals Bt1, Bt2, Bt4, and Bt5) from sample DM1540 show significantly different age spectra, characterized by a saddle shape, suggesting a two–stage heterogeneous trapping process, differently from sample DM1517. In the case of biotite separated from the metagranites by Tilton et al. (1997), the age spectra from multi crystals give the troughs between 900–971 °C for two samples, suggesting a homogeneous trapping process.

The observed variation of the biotite age spectra among samples DM1517 and DM1540, and the sample studied by Tilton et al. (1997) may reflect different trapping processes of EAW and/or localized source of EAW. In all the cases, the extremely high excess argon in biotites could be due to the extremely fast exhumation of the BIU and the surrounding Pinerolo and Rocca Solei Units (cf. Rubatto and Hermann, 2001) as the extremely high excess argon pressure could happen in the units by the radiogenic argon release from the deformed white micas in extremely short time during the extremely fast exhumation.

ACKNOWLEDGMENTS

We thank Kazumasa Aoki who helped us for the EMP analyses. The JSPS Grant–in–Aid for Scientific Research #20244087 financially supported in part this research for T. Itaya. The neutron irradiation experiment was carried out in the visiting researcher program in Kyoto University Reactor (KUR). We thank staffs of Kyoto University, especially K. Takamiya for his help in the course of experiment. We acknowledge two reviewers who critically reviewed the first manuscript and are also grateful for M. Satish–Kumar's efforts editing the final manuscript for clarity.

SUPPLEMENTARY MATERIAL

Supplementary Table and color version of Figures 2 and 3 are available online from https://doi.org/10.2465/jmps.171201.

REFERENCES

Arnaud, N.O. and Kelley, S.P. (1995) Evidence for excess argon during high pressure metamorphism in the Dora Maira (western Alps, Italy), using an ultra-violet laser ablation microprobe ^{40}Ar–^{39}Ar technique. Contributions to Mineralogy and Petrology, 121, 1-11.

Avigad, D., Chopin, C. and Le Bayon, R. (2003) Thrusting and extension in the southern Dora-Maira ultra-high pressure massif (Western Alps): view from below the coesite-bearing unit. Journal of Geology, 111, 57-70.

Beltrando, M., Di Vincenzo, G. and Ferraris, C. (2013) Preservation of sub-microscopic structural relics in micas from the Gran Paradiso Massif (Western Alps): Implications for ^{40}Ar-^{39}Ar geochronology. Geochimica et Cosmochimica Acta, 119, 359-380.

Chopin, C. and Maluski, H. (1980) ^{40}Ar–^{39}Ar dating of high pressure metamorphic micas from the Gran Paradiso area (Western Alps): Evidence against the blocking temperature concept. Contributions to Mineralogy and Petrology, 74, 109-122.

Chopin, C., Henry, C. and Michard, A. (1991) Geology and petrology of the coesite-bearing terrane, Dora Maira massif, Western Alps. European Journal of Mineralogy, 3, 263-291.

Compagnoni, R., Rolfo, F., Groppo, C., Hirajima, T. and Turello, R. (2012) Geological map of the ultra-high pressure Brossasco-Isasca unit (Western Alps, Italy). Journal of Maps, 8, 465-472.

De Jong, K., Féraud, G., Ruffet, G., Amouric, M. and Wijbrans, J.R. (2001) Excess argon incorporation in phengite of the Mulhacén Complex: submicroscopic illitization and fluid ingress during late Miocene extension in the Betic Zone, southeastern Spain. Chemical Geology, 178, 159-195.

Di Vincenzo, G., Tonarini, S., Lombardo, B., Castelli, D. and Ottolini, L. (2006) Comparison of ^{40}Ar–^{39}Ar and Rb-Sr data on phengites from the UHP Brossasco-Isasca Unit (Dora Maira Massif, Italy): Implications for dating white mica. Journal of Petrology, 47, 1439-1465.

Duchêne, S., Blichert-Toft, J., Luais, B., Télouk, P., Lardeaux, J.-M. and Albarède, F. (1997). The Lu-Hf dating of garnets of the Alpine high- pressure metamorphism. Nature, 387, 586-589.

Ferrando, S., Frezzotti, M.L., Petrelli, M. and Compagnoni, R. (2009) Metasomatism of continental crust during subduction: the UHP whiteschists from the Southern Dora-Maira Massif (Italian Western Alps). Journal of Metamorphic Geology, 27, 739-756.

Gebauer, D., Schertl, H.-P., Brix, M. and Schreyer, W. (1997) 35 Ma old ultrahigh-pressure metamorphism and evidence for very rapid exhumation in the Dora Maira Massif, Western Alps. Lithos, 41, 5-24.

Giorgis, D., Coscam, M. and Li, S. (2000) Distribution and significance of extraneous argon in UHP eclogite (Sulu terrain, China): Insight from in situ $^{40}Ar/^{39}Ar$ UV laser ablation analysis. Earth and Planetary Science Letter, 181, 605-15.

Gouzu, C., Itaya, T., Hyodo, H. and Ahmad, A.T. (2006) Cretaceous isochron ages from K-Ar and Ar-Ar dating of eclogitic rocks in the Tso Morari complex, western Himalaya, India. Gondwana Research, 9, 426-440.

Gouzu, C., Yagi, K., Thanh, N.X., Itaya, T. and Compagnoni, R. (2016) White mica K-Ar geochronology of HP-UHP units in the Lago di Cignana area, western Alps, Italy: Tectonic implications for exhumation. Lithos, 248-251, 109-118.

Halama, R., Konrad-Schmolke, M., Sudo, M., Marschall, H.R. and Wiedenbeck, M. (2014) Effects of fluid-rock interaction on $^{40}Ar/^{39}Ar$ geochronology in high-pressure rocks (Sesia-Lanzo Zone, Western Alps). Geochimica et Cosmochimica Acta, 126, 475-494.

Hammerschmidt, K., Schertl, H.P., Friedrichsen, H. and Schreyer, W. (1995) Excess Ar a common feature in ultrahigh-pressure rocks: a case study on micas from the Dora-Maira Massif, western Alps, Italy. Terra Nova, 7, 349.

Hyodo, H. and York, D. (1993) The discovery and significance of a fossilized radiogenic argon wave (argonami) in the earth's crust. Geophysical Research Letter, 2011, 61-64.

Hyodo, H., Matsuda, T., Fukui, S. and Itaya, T. (1994) $^{40}Ar/^{39}Ar$ age determination of a single mineral grain by Laser step heating. Bulletin of Research Institute of Natural Sciences, Okayama University of Science, 20, 63-67 (in Japanese with English Abstract).

Hyodo, H., Itaya, T. and Matsuda, T. (1995) Temperature measurement of small minerals and its precision using Laser heating. Bulletin of Research Institute of Natural Sciences, Okayama University of Science, 21, 3-6 (in Japanese with English Abstract).

Hyodo, H., Kim, S., Itaya, T. and Matsuda, T. (1999) Homogeneity of neutron flux during irradiation for $^{40}Ar/^{39}Ar$ age dating in the research reactor at Kyoto University. Journal of Mineralogy and Petrological Sciences, 94, 329-337.

Itaya, T., Hyodo, H., Uruno, K. and Mikoshiba, M.-U. (2005) Ultra-high excess argon in kyanites: Implications for ultra-high pressure metamorphism in Northern Japan. Gondwana Research, 8, 617-621.

Itaya, T., Hyodo, H., Tsujimori, T., Wallis, S., Aoya, M., Kawakami, T. and Gouzu, C. (2009) Regional-Scale Excess Ar wave in a Barrovian type metamorphic belt, eastern Tibetan Plateau. Island Arc, 18, 293-305.

Itaya, T., Tsujimori, T. and Liou, J.G. (2011) Evolution of the Sanbagawa and Shimanto high-pressure belts in SW Japan: Insights from K-Ar (Ar-Ar) geochronology. Journal of Asian Earth Sciences, 42, 1075-1090.

Itaya, T. and Tsujimori, T. (2015) White mica K-Ar geochronology of the Sanbagawa eclogites in SW Japan: Implications on deformation-controlled K-Ar closure temperature. International Geology Review, 57, 1014-1022.

Itaya, T., Yagi, K., Gouzu, C., Thanh, N.X. and Groppo, C. (2017) Preliminary report on the excess argon bearing Orthoclase from metagranite in the Brossasco-Isasca UHP Unit of Dora-Maira Massif, Italy. Journal of Mineralogy and Petrological Sciences, 112, 36-39.

Jahn, B.M., Caby, R. and Monié, P. (2001) The oldest UHP eclogites of the World: age of UHP metamorphism, nature of protoliths and tectonic implications. Chemical Geology, 178, 143-158.

Kaneoka, I. and Takaoka, N. (1980) Rare gas isotopes in Hawaiian ultramafic nodules and volcanic rocks: Constraint on genetic relationships. Science, 208, 1366-1368.

Li, S., Wang, S., Chen, Y., Liu, D., Qiu, J., Zhou, H. and Zhang, Z. (1994) Excess argon in phengite from eclogite: Evidence from dating of eclogite minerals by Sm-Nd, Rb-Sr and $^{40}Ar/^{39}Ar$ methods. Chemical Geology, 112, 343-350.

Matsumoto, N. and Hirajima, T. (2000) Garnet in pelitic schists from a quartz-eclogite unit of the southern Dora-Maira massif, Western Alps. Schweizerische mineralogische und petrographische Mitteilungen, 80, 53-62.

Monié, P. and Chopin, C. (1991) $^{40}Ar/^{39}Ar$ dating in coesite-bearing and associated units of the Dora Maira massif, Western Alps. European Journal of Mineralogy, 3, 239-262.

Roddick, J.C. (1983) High precision intercalibration of ^{40}Ar-^{39}Ar standards. Geochimica et Cosmochimica Acta, 47, 887-898.

Rubatto, D. and Hermann, J. (2001) Exhumation as fast as subduction? Geology, 29, 3-6.

Scaillet, S., Féraud, G., Lagabrielle, Y., Ballévre, M. and Ruffet, G. (1990) $^{40}Ar/^{39}Ar$ laser-probe dating by step-heating and spot-fusion of phengites from the Dora Maira nappe of the western Alps, Italy. Geology, 18, 741-744.

Scaillet, S., Féraud, G., Ballévre, M. and Amouric, M. (1992) Mg/Fe and [(Mg,Fe)Si-Al2] compositional control on Ar behaviour in high-pressure white micas: a $^{40}Ar/^{39}Ar$ continuous laser-probe study from the Dora-Maira nappe of the internal western Alps, Italy. Geochimica et Cosmochimica Acta, 56, 2851-2872.

Scaillet, S. (1996) Excess ^{40}Ar transport scale and mechanism in high-pressure phengites; A case study from an eclogitized metabasite of the Dora-Maira nappe, western Alps. Geochimica et Cosmochimica Acta, 60, 1075-1090.

Schertl, H-P. and Hammerschmidt, K. (2016) Tracking the incidence of excess argon in white mica Ar-Ar data from UHP conditions to upper crustal levels in the Dora-Maira Massif, Western Alps. European Journal of Mineralogy, 28, 1255-1275.

Sherlock, S.C. and Arnaud, N.O. (1999) Flat plateau and impossible isochrons: Apparent ^{40}Ar-^{39}Ar geochronology in a high-pressure terrain. Geochimica et Cosmochimica Acta, 63, 2835-2838.

Tilton, G.R., Ames, L., Schertl, H.-P. and Schreyer, W. (1997) Reconnaissance isotopic investigations on rocks of an underformed granite contact within the coesite-bearing unit of the Dora Maira Massif. Lithos, 41, 25-36.

Tonarini, S., Villa, I.M., Oberli, F., Meier, M., Spencer, D.A., Pognante, U. and Ramsay, J.G. (1993) Eocene age of eclogite metamorphism in Pakistan Himalaya: Implications for India-Eurasian collision. Terra Nova, 5, 13-20.

Wanless, R.K., Stevens, R.D. and Loveridge, W.D. (1970) Anomalous parent-daughter isotopic relationships in rocks adjacent to the Grenville Front near Chibougamau, Quebec. Eclogae Geol. Helv., 63, 345-364.

Manuscript received December 1, 2017
Manuscript accepted April 18, 2018
Published online August 25, 2018
Manuscript handled by M. Satish-Kumar